End Stages of Stellar Evolution, I

Stars end their life as one of three kinds of different compact objects:

End Stages of Stellar Evolution, II

Stars end their life as one of three kinds of different compact objects:

White Dwarf: $\rho \sim 10^5 \dots 10^6\,\mathrm{g\,cm^{-3}}$, $R \sim R_\oplus$, Equilibrium between gravitation and pressure from degenerate electrons, $M < 1.44\,M_\odot$ (Chandrasekhar-limit; 1931).

End Stages of Stellar Evolution, III

Stars end their life as one of three kinds of different compact objects:

White Dwarf: $\rho \sim 10^5 \ldots 10^6\,\mathrm{g\,cm^{-3}}$, $R \sim R_\oplus$, Equilibrium between gravitation and pressure from degenerate electrons, $M < 1.44\,M_\odot$ (Chandrasekhar-limit; 1931).

Neutron Star: $\rho \sim 10^{13} \ldots 10^{16}\,\mathrm{g\,cm^{-3}}$, $R \sim 10\,\mathrm{km}$, this density causes inv. β-decay ($\mathrm{p} + \mathrm{e}^- \rightarrow \mathrm{n}$), i.e., star consists (mainly) of neutrons. $1.44\,M_\odot < M \lesssim 3\,M_\odot$ (Oppenheimer-Volkoff limit; 1939).

End Stages of Stellar Evolution, IV

Stars end their life as one of three kinds of different compact objects:

White Dwarf: $\rho \sim 10^5 \ldots 10^6\,\mathrm{g\,cm^{-3}}$, $R \sim R_\oplus$, Equilibrium between gravitation and pressure from degenerate electrons, $M < 1.44\,M_\odot$ (Chandrasekhar-limit; 1931).

Neutron Star: $\rho \sim 10^{13} \ldots 10^{16}\,\mathrm{g\,cm^{-3}}$, $R \sim 10\,\mathrm{km}$, this density causes inv. β-decay ($\mathrm{p} + \mathrm{e}^- \rightarrow \mathrm{n}$), i.e., star consists (mainly) of neutrons. $1.44\,M_\odot < M \lesssim 3\,M_\odot$ (Oppenheimer-Volkoff limit; 1939).

Black Hole: For $M \gtrsim 3\,M_\odot$ no stable configuration known

$\Longrightarrow$ Star collapses completely

$\Longrightarrow$ Black Hole

Size scale: $R_\mathrm{S} = 2GM/c^2 = 3(M/M_\odot)\,\mathrm{km}$

Detectability, I

Sirius A+B (McDonald Observatory)

Luminosity of a sphere of radius R and temperature T:

$$L = 4\pi R^2 \cdot \sigma_{\mathrm{SB}} T^4 \qquad (3.1)$$

($\sigma_{\mathrm{SB}} = 5.67 \times 10^{-5}\,\mathrm{erg\,cm^{-2}\,K^{-4}\,s^{-1}}$)

For a typical white dwarf,
$R \sim 6000\,\mathrm{km}$, $T \sim 10000\,\mathrm{K}$
$\Longrightarrow L = 2.6 \times 10^{30}\,\mathrm{erg\,s^{-1}} \sim 6.6 \times 10^{-4}\,L_\odot$ corresponding to an absolute magnitude of $M_{\mathrm{WD}} = 15.9\,\mathrm{mag}$.

$\Longrightarrow$ with a limiting magnitude of 25 mag for today's telescopes, isolated WDs are detectable out to $\sim$700 pc.

First discovery: Alvan Graham Clark, 1862

Detectability, II

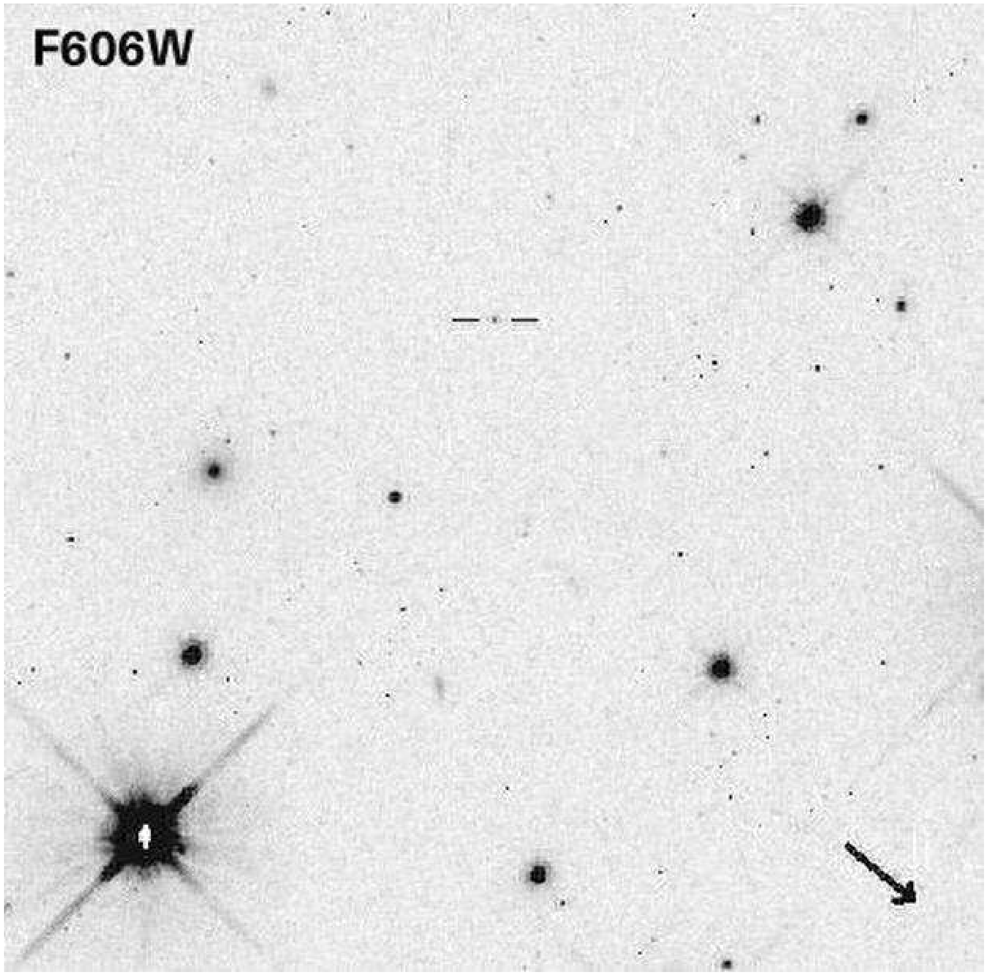

(17.5′ × 17.5′ Walter & Matthews, 1997, Fig. 1)

Same calculation for a neutron star ($R = 10$ km, $T = 10^6$ K) gives $L_{\mathrm{NS}} \sim 7 \times 10^{28}$ erg s $\sim 2 \times 10^{-5}\, L_{\odot}$, or an absolute magnitude of 19.7 mag.

Pre VLT/Keck: practical limit of surveys ~20 pc, 10 m class and space based telescopes of today extend this to ~100 pc.

$\Longrightarrow$ It is virtually impossible to discover isolated neutron stars in the optical.

HST Image of the isolated neutron star RX J185635−3754, which has a visual magnitude ~25.6 mag

Detectability, III

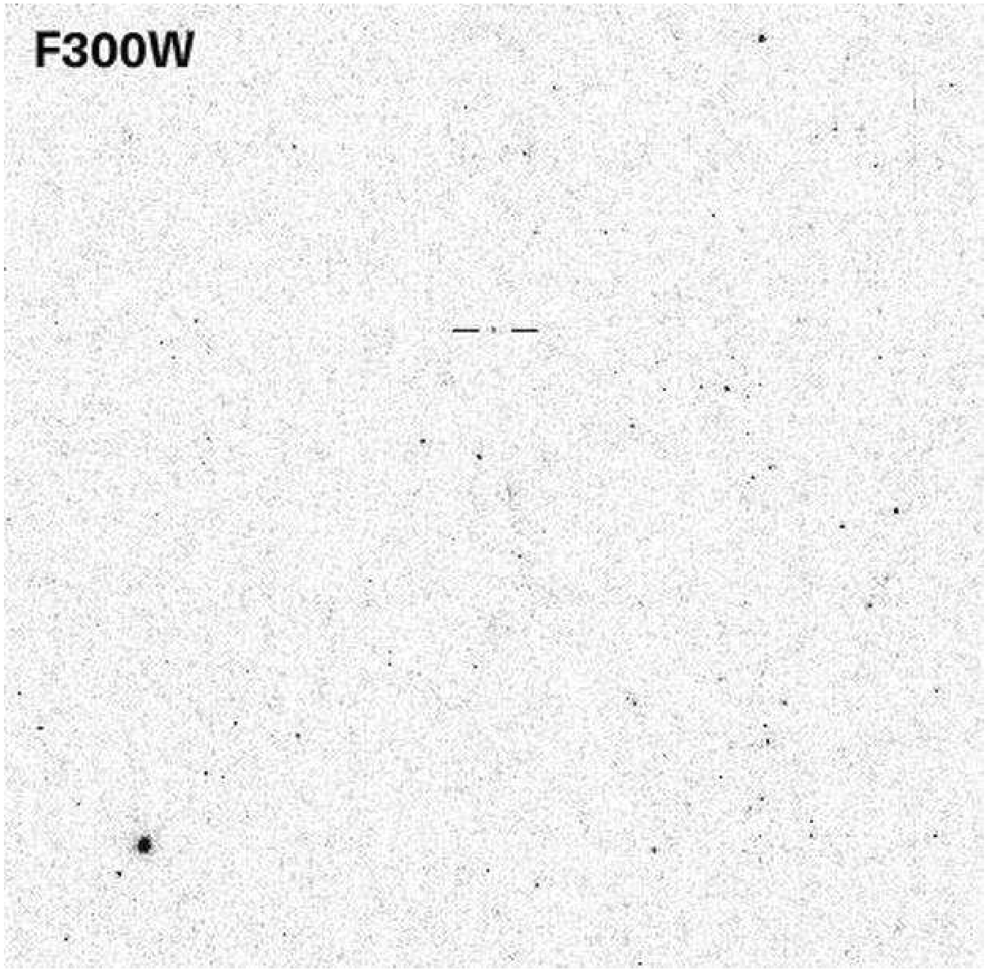

(17.5′ × 17.5′ Walter & Matthews, 1997, Fig. 1)

Same calculation for a neutron star ($R = 10\,\mathrm{km}$, $T = 10^6\,\mathrm{K}$) gives $L_{\mathrm{NS}} \sim 7 \times 10^{28}\,\mathrm{erg\,s} \sim 2 \times 10^{-5}\,L_{\odot}$, or an absolute magnitude of 19.7 mag.

Pre VLT/Keck: practical limit of surveys ∼20 pc, 10 m class and space based telescopes of today extend this to ∼100 pc.

$\Longrightarrow$ It is virtually impossible to discover isolated neutron stars in the optical.

HST Image of the isolated neutron star RX J185635−3754, which has a visual magnitude ∼25.6 mag

What are XRBs?, I

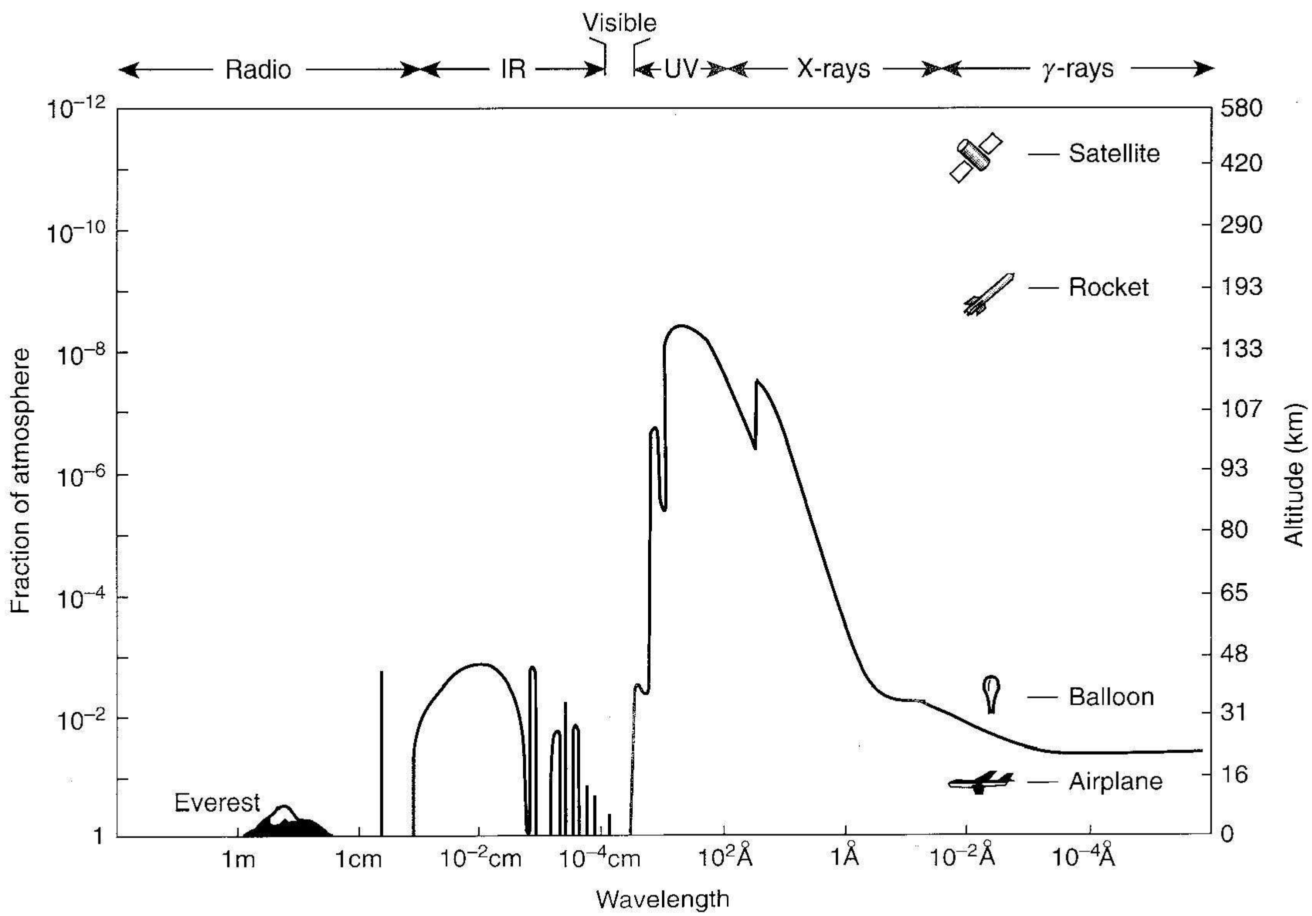

Earth's atmosphere is opaque for all types of EM radiation except for optical light and radio.

1940s: first opening of other wavebands than the optical: radio and X-rays

1948: first detection of X-rays from Sun from (modified V2 rocket; Friedman et al.)

(Charles & Seward, 1995, Fig. 1.12)

Sun's relative weakness stopped search for other cosmic X-ray sources for 13 years.

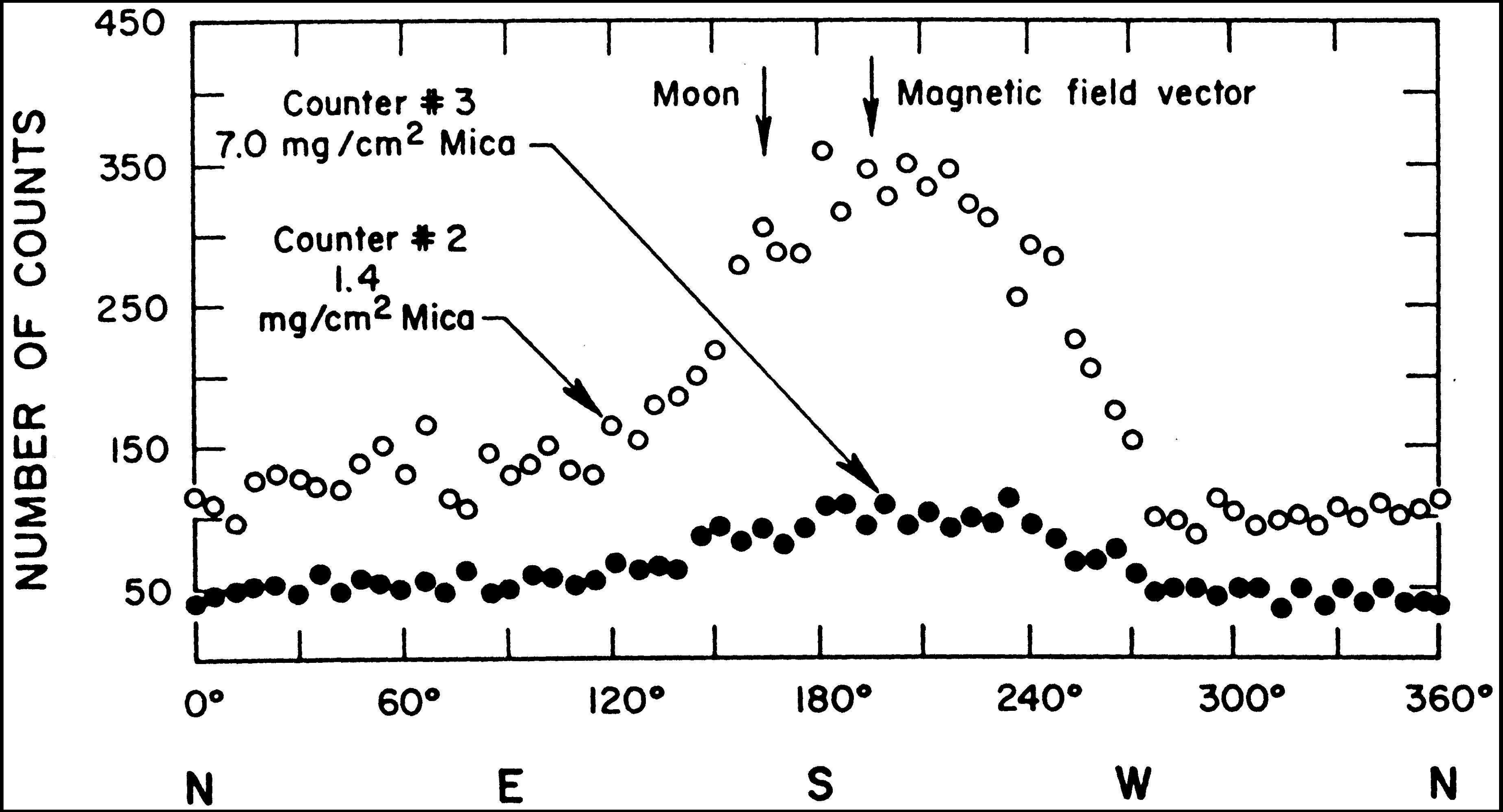

Early 1960s: First X-ray observations of the sky with collimated Geiger counters

(Riccardo Giacconi et al. at American Science & Engineering, Boston, prompted by B. Rossi):

Search for X-ray fluorescence emission from the Moon

18 June 1962: 1st scan of the sky during an Aerobee flight (Giacconi et al., 1962):

First discovery of an extrasolar X-ray source – Sco X-1

Nobel prize in 2002 to R. Giacconi

The moon was fi rst detected in the X-rays by *ROSAT* in the 1990s.

What are XRBs?, III

Throughout the 1960s further detections of X-ray sources with X-ray detectors using rocket flights:

- 18 June 1962: Sco X-1 (Giacconi et al., 1962) [AS&E]
- 29 April 1963: Crab nebula (Bowyer et al., 1964) [NRL]
- 16 June 1964: Cygnus X-1 (Bowyer et al., 1965)
- 16 June 1964: Galactic Center (Bowyer et al., 1965)
- 16 June 1964: SN 1604 (Kepler's SNR Bowyer et al., 1965)
- . . .

Some sources were speculated to be neutron stars

confirmation of these observations by teams from MIT (Clark, Oda), Lawrence Livermore Laboratory (Chodil et al.), Leicester (Pounds et al.), and others.

End of 1960s: $\sim$60 sources known.

Problems of rocket and balloon studies: pointing accuracy, short observing time.

To be able to have longer observing times, one needs to go to space!

UHURU

NASA/GSFC

12 Dec 1970: launch of *UHURU*:

First satellite sensitive to X-rays

UHURU: Swahili for “freedom”

Detailed observations/positions for many bright X-ray sources (e.g., Cygnus X-1, Hercules X-1, etc.), discovery of many more

Discovered sources summarized in the 4th *UHURU* catalog (339 sources, Forman et al. 1978).

Source names: e.g., 4U0115+63, 4U1957+11,. . .

Discovery of X-ray Binaries, I

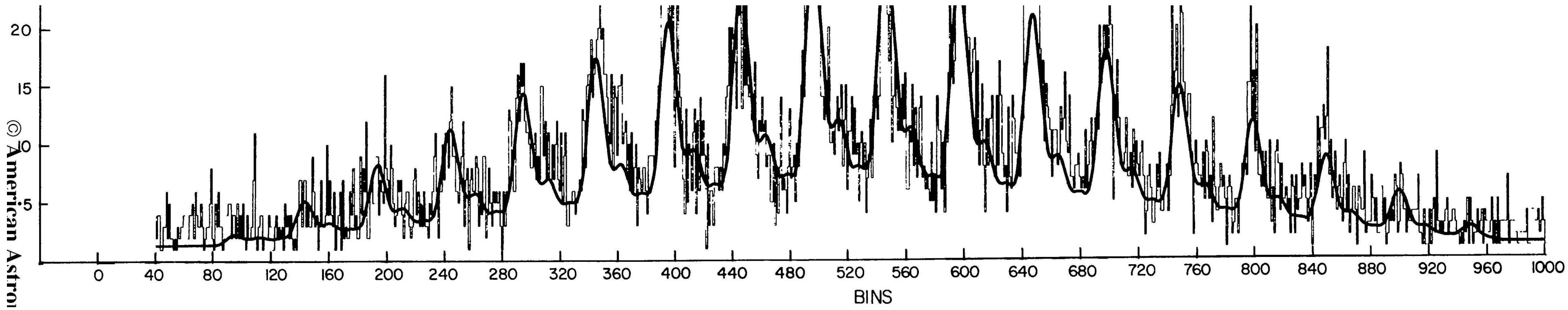

(Schreier et al., 1972, Fig. 4a)

Schreier et al. (1972): Detection of 4.8 s pulsations from Centaurus X-3 with *UHURU*: Cen X-3 is an X-ray Pulsar.

$\Longrightarrow$ at least some X-ray sources are rotating.

Discovery of X-ray Binaries, II

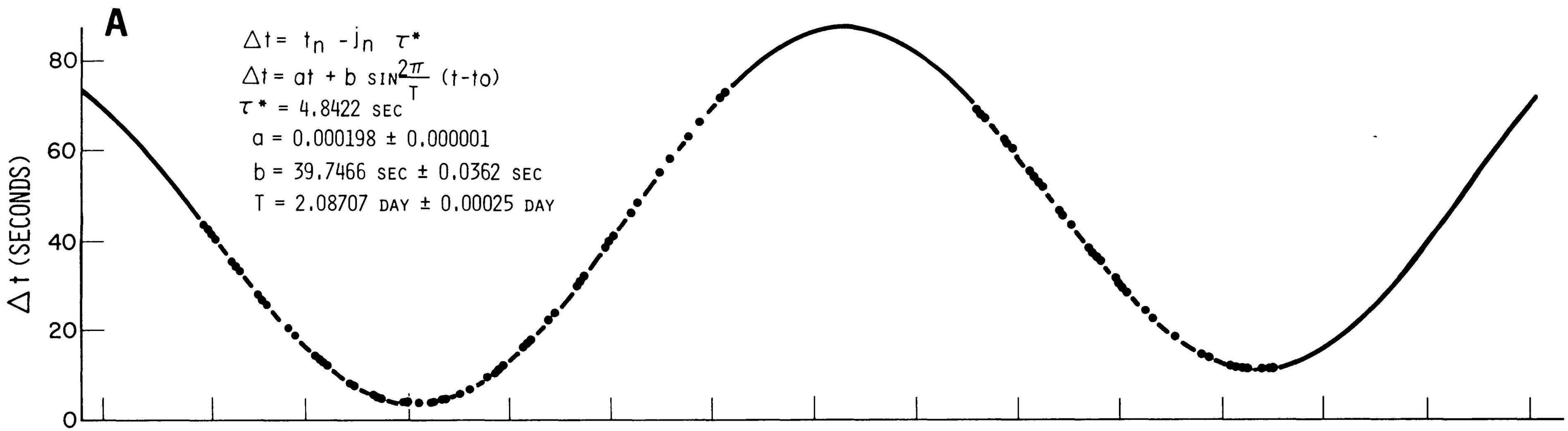

(Schreier et al., 1972, Fig. 4a)

Schreier et al. (1972): Time delay in arrival time of pulses from Cen X-3:

Cen X-3 is an X-ray Pulsar.

Discovery of X-ray Binaries, III

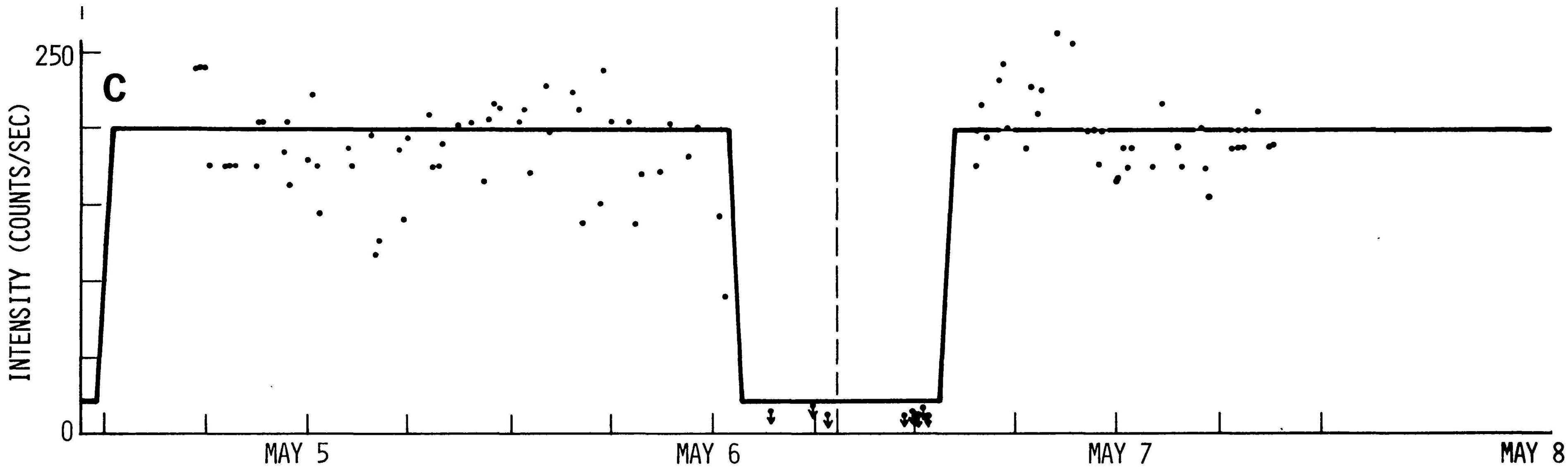

FIG. 4.—*Continued*

(Schreier et al., 1972, Fig. 4c)

Schreier et al. (1972): Cen X-3 shows periodic drops in X-ray count rate on a timescale of 2.08 d.

$\Longrightarrow$ eclipses by a star?

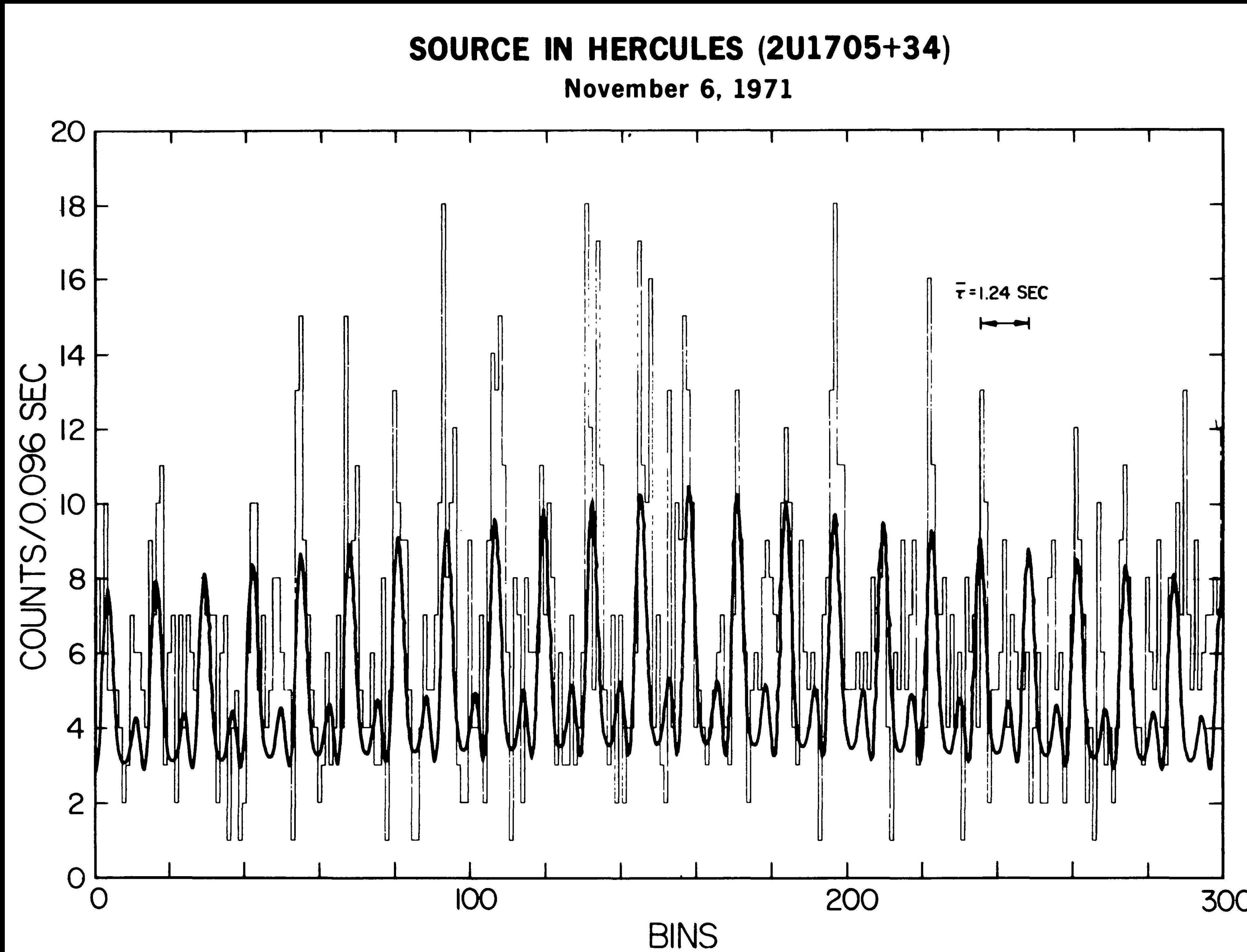

(Tananbaum et al., 1972, Fig. 1)

Detection of 1.24 s pulsations from Hercules X-1 with *UHURU*:

$\Longrightarrow$ X-ray pulsars as class of objects

Discovery of X-ray Binaries, V

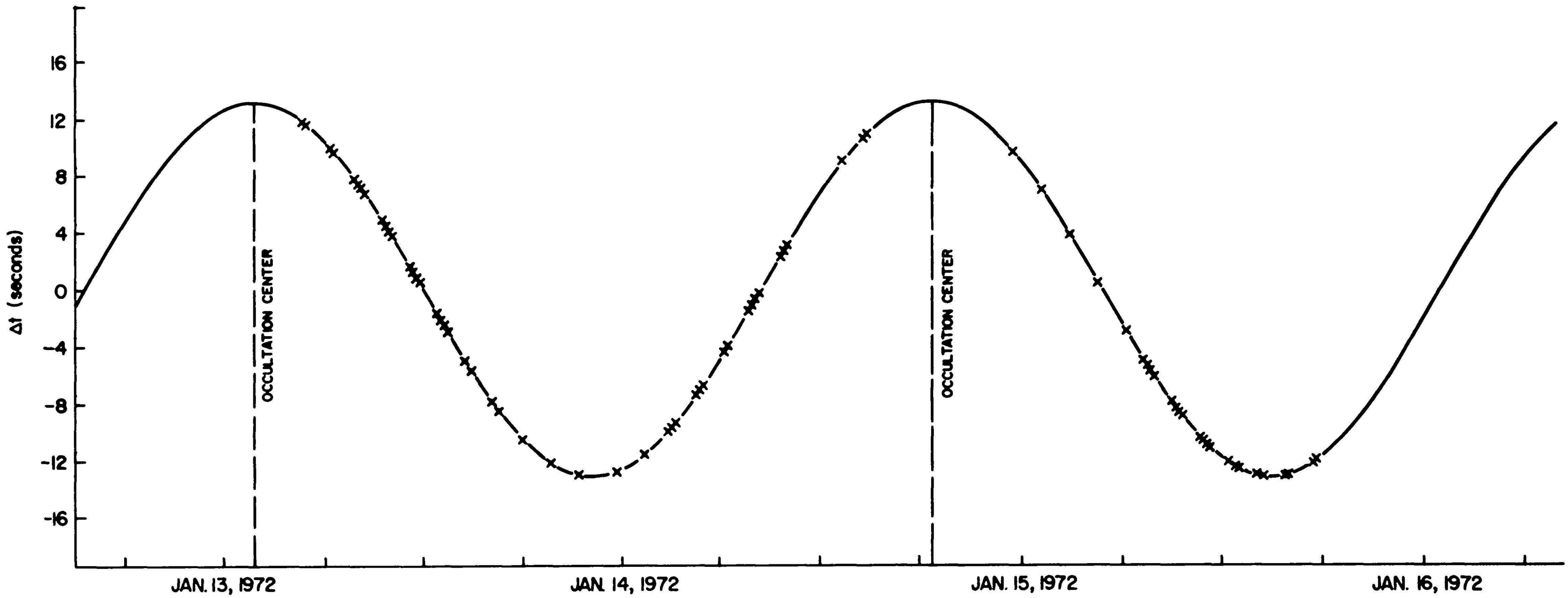

(Tananbaum et al., 1972, Fig. 3)

Similar to Cen X-3, X-ray pulsations of Her X-1 show periodic delays

(timescale: 1.7 d)

$\Longrightarrow$ X-ray binaries as class of objects

The observed amplitude of the time delays seen in Her X-1 is ± 13.19 s. Since it is sinusoidal the X-ray emitting object is very likely to move on a circular orbit together with the optical star around their center of mass (CM).

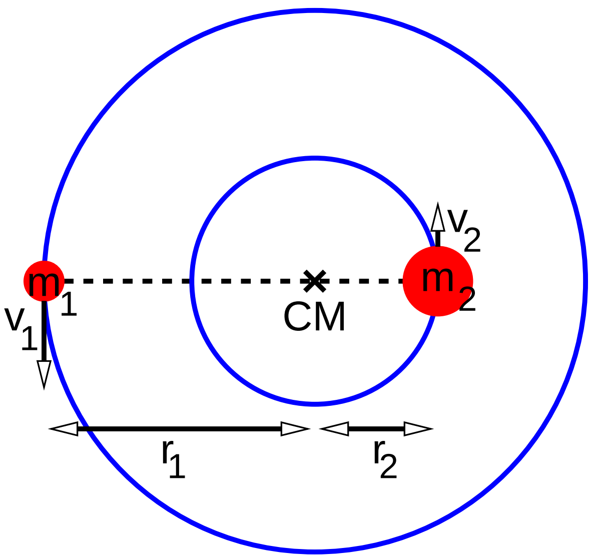

The distances from the CM are given by

$$m_1 r_1 = m_2 r_2 = m_2 (r - r_1) \tag{3.2}$$

where $r = r_1 + r_2$. Therefore

$$m_1 r_1 + m_2 r_1 = m_2 r \quad \Longrightarrow r_1 = \frac{m_2 r}{m_1 + m_2} \tag{3.3}$$

The velocity of object 1 is then

$$v_1 = \frac{2\pi r_1}{P} \tag{3.4}$$

where P is the observed period.

The observed velocity component (perpendicular to the plane of sky) is

$$v_{1,\mathrm{obs}} = v_1 \sin i = \frac{2\pi r_1}{P} \sin i = \frac{2\pi r}{P} \frac{m_2}{m_1 + m_2} \sin i \tag{3.5}$$

where i is the system's inclination ($i = 90^\circ$ is an "edge on orbit").

To replace r with observables, we derive Kepler's 3rd law for the special case of a circular orbit where the centripetal force is balanced by the gravitational force:

$$\frac{m_1 v_1^2}{r_1} = G \frac{m_1 m_2}{r^2} \tag{3.6}$$

Therefore, inserting v_1 from above

$$\frac{4\pi^2}{P^2} \frac{r}{m_1 + m_2} = G \frac{m_2}{r^2} \quad \Longrightarrow \quad \frac{r^3}{P^2} = \frac{G}{4\pi^2}(m_1 + m_2) \tag{3.7}$$

We can now use Eq. (3.7) to eliminate r in Eq. (3.5):

First, solve Eq. (3.5) for r/P...

$$\frac{r}{P} = \frac{v_{1,\mathrm{obs}}}{2\pi} \frac{m_1 + m_2}{m_2} \frac{1}{\sin i} \tag{3.8}$$

take the cube of this equation...

$$\frac{r^3}{P^3} = \frac{v_{1,\text{obs}}^3}{8\pi^3}\frac{(m_1+m_2)^3}{m_2^3}\frac{1}{\sin^3 i} \tag{3.9}$$

insert Eq. (3.7)...

$$\frac{G}{4\pi^2}(m_1+m_2) = \frac{Pv_{1,\text{obs}}^3}{8\pi^3}\frac{(m_1+m_2)^3}{m_2^3}\frac{1}{\sin^3 i} \tag{3.10}$$

and move all known quantities to one side of the $=$-sign to obtain the mass function:

$$\frac{m_2^3\sin^3 i}{(m_1+m_2)^2} = \frac{Pv_1^3}{2\pi G} := f_M \tag{3.11}$$

Note that the mass function gives a *lower limit* for m_2 when the velocity amplitude of the other object, v_1, has been observed.

For the case of Hercules X-1, the observed time delay is $\Delta t = 13.19\,s$. This corresponds to an orbital radius of $r_1 = c\Delta t = 4\times 10^6$ km and the velocity is $v_1 \sim 170\,\text{km}\,\text{s}^{-1}$. Since eclipses have been observed in Her X-1, the inclination is $i = 90^\circ$. Therefore, the mass function of Her X-1 becomes $f_M = 1.75\times 10^{33}\,\text{g} = 0.876\,M_\odot$.

Discovery of X-ray Binaries, VI

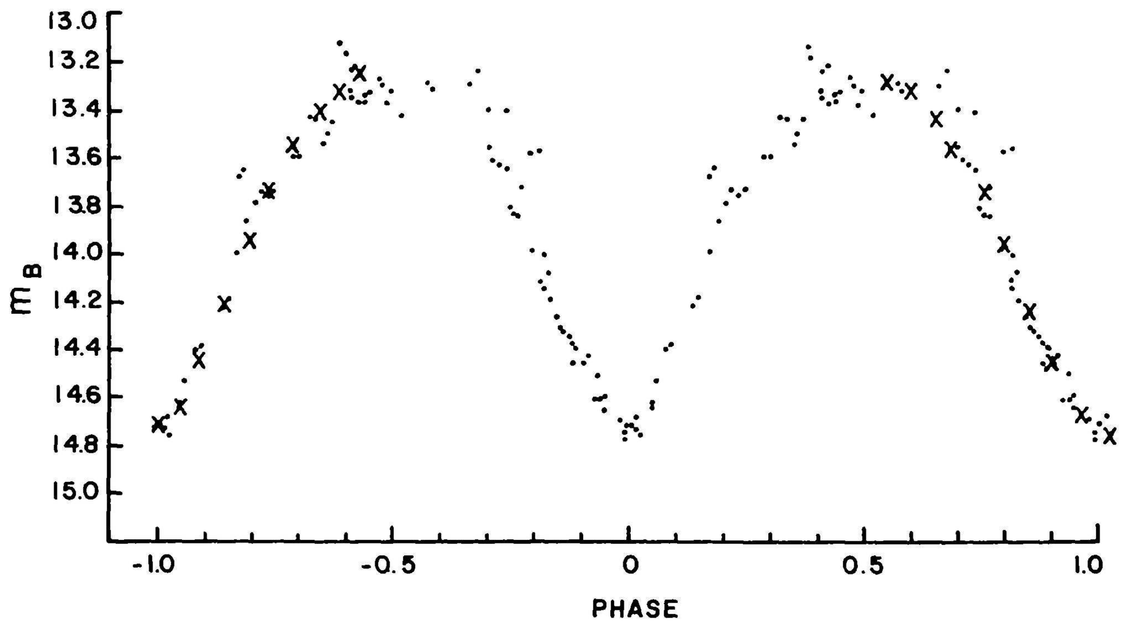

(Bahcall & Bahcall, 1972, Fig. 2)

Shortly after the *UHURU* measurements, HZ Her was identified as the optical companion, which is varying on the 1.7 d orbital period.

HZ Her was recognized as a variable star by C. Hoffmeister in 1936.

This allowed the mass of the companion to be measured to $m_2 = 2.3\,M_\odot$, and the mass of the X-ray source to $m_1 = 1.4\,M_\odot$.

Her X-1 is a neutron star.

Black Hole Binaries, I

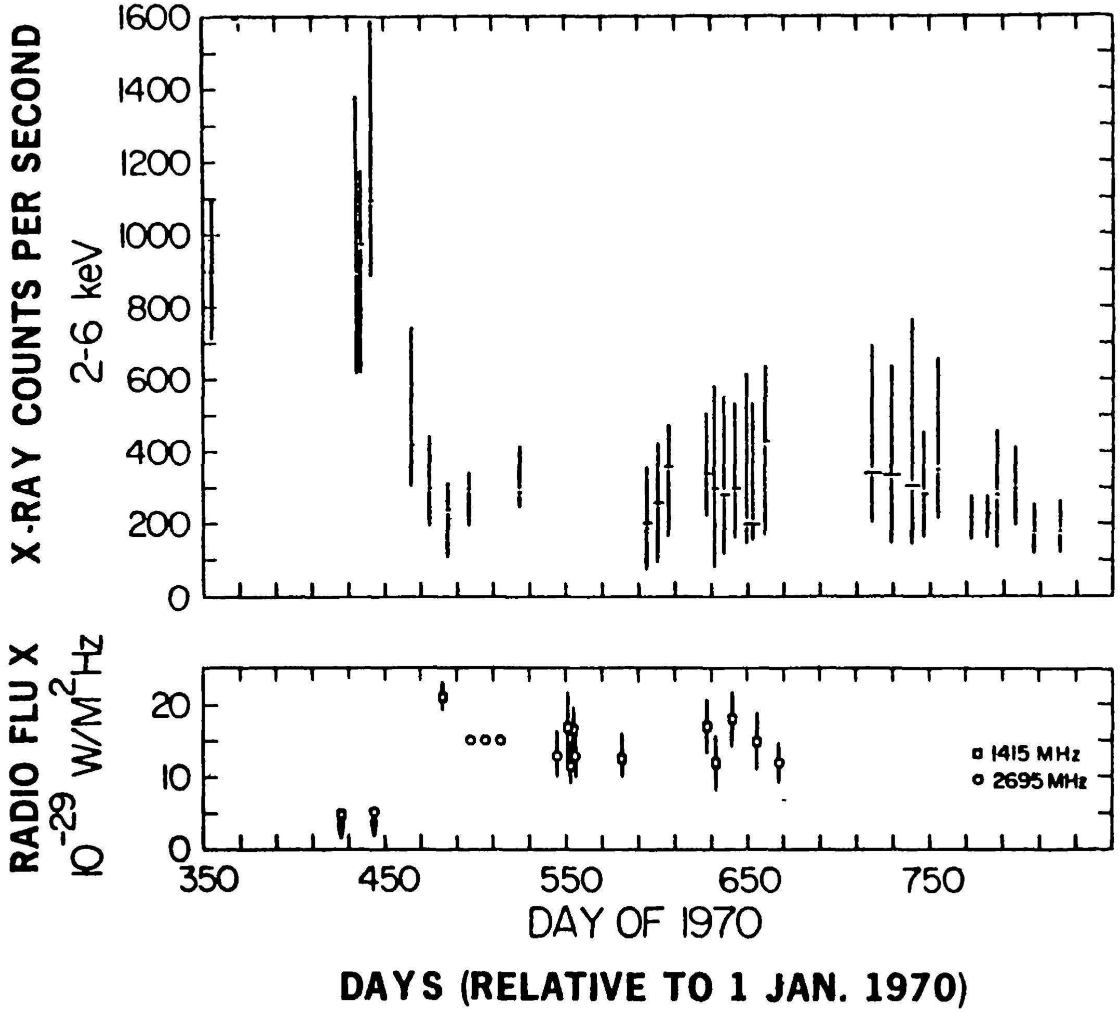

In Cyg X-1, no coherent periodicities were found.

However, Cyg X-1 showed correlated behavior in the radio and in the X-rays

$\Longrightarrow$ source localization, counterpart is HDE 226868, an O-star

(Murdin & Webster, 1971; Hjellming & Wade, 1971)

Black Hole Binaries, II

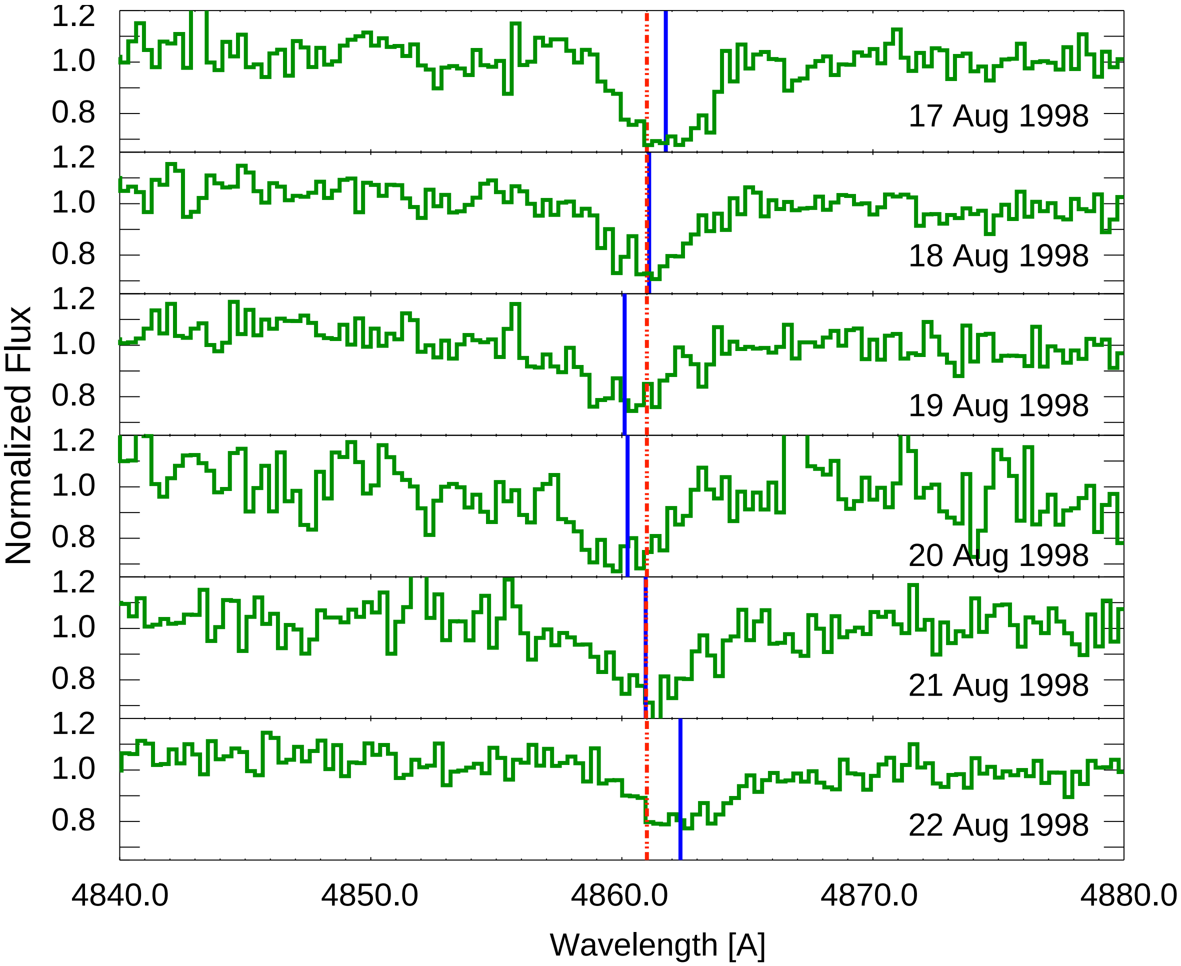

Motion of the Hβ line in HDE 226868/Cyg X-1 (Pottschmidt, Wilms)

For Cygnus X-1, the mass function is $f_M = 0.252\,M_\odot$, however, the companion is an O-star with $> 10\,M_\odot$, and this puts a lower limit of $\sim 8\,M_\odot$ to the mass of the compact object (Webster & Murdin, 1972)

The X-ray emitting object in Cygnus X-1 is a black hole.

Accretion, I

Why are X-ray binaries so bright?

1. Fusion

Reactions à la

$$4\mathrm{p} \longrightarrow {}^{4}\mathrm{He} + \Delta mc^2$$

Energy released:

Fusion yields
$\sim 6 \times 10^{18}\,\mathrm{erg\,g^{-1}} = 6 \times 10^{11}\,\mathrm{J\,g^{-1}}$

($\Delta E_{\mathrm{nuc}} \sim 0.007 m_{\mathrm{p}} c^2$)

Accretion, II

Why are X-ray binaries so bright?

1. Fusion

Reactions à la

$$4\mathrm{p} \longrightarrow {}^4\mathrm{He} + \Delta mc^2$$

Energy released:

Fusion yields
$\sim 6 \times 10^{18}\,\mathrm{erg\,g^{-1}} = 6 \times 10^{11}\,\mathrm{J\,g^{-1}}$

($\Delta E_{\mathrm{nuc}} \sim 0.007 m_{\mathrm{p}} c^2$)

2. Gravitation

Accretion of mass m from ∞ onto Black Hole M with radius R_{S} yields

$$\Delta E_{\mathrm{acc}} = \frac{GMm}{R_{\mathrm{S}}} \quad \text{where} \quad R_{\mathrm{S}} = \frac{2GM}{c^2}$$

Accretion produces
$\sim 10^{20}\,\mathrm{erg\,g^{-1}} = 10^{13}\,\mathrm{J\,g^{-1}}$

($\Delta E_{\mathrm{acc}} \sim 0.1\, m_{\mathrm{p}} c^2$)

Accretion, III

Why are X-ray binaries so bright?

1. Fusion

Reactions à la

$$4\mathrm{p} \longrightarrow {}^4\mathrm{He} + \Delta mc^2$$

Energy released:

$\boxed{\text{Fusion yields } \sim 6 \times 10^{18}\,\mathrm{erg\,g^{-1}} = 6 \times 10^{11}\,\mathrm{J\,g^{-1}}}$

($\Delta E_{\mathrm{nuc}} \sim 0.007 m_{\mathrm{p}} c^2$)

2. Gravitation

Accretion of mass m from ∞ onto Black Hole M with radius R_{S} yields

$$\Delta E_{\mathrm{acc}} = \frac{GMm}{R_{\mathrm{S}}} \quad \text{where} \quad R_{\mathrm{S}} = \frac{2GM}{c^2}$$

$\boxed{\text{Accretion produces } \sim 10^{20}\,\mathrm{erg\,g^{-1}} = 10^{13}\,\mathrm{J\,g^{-1}}}$

($\Delta E_{\mathrm{acc}} \sim 0.1\, m_{\mathrm{p}} c^2$)

$\Longrightarrow$ Accretion of material is the most efficient astrophysical energy source.

...therefore accreting objects are the most luminous objects in the whole universe.

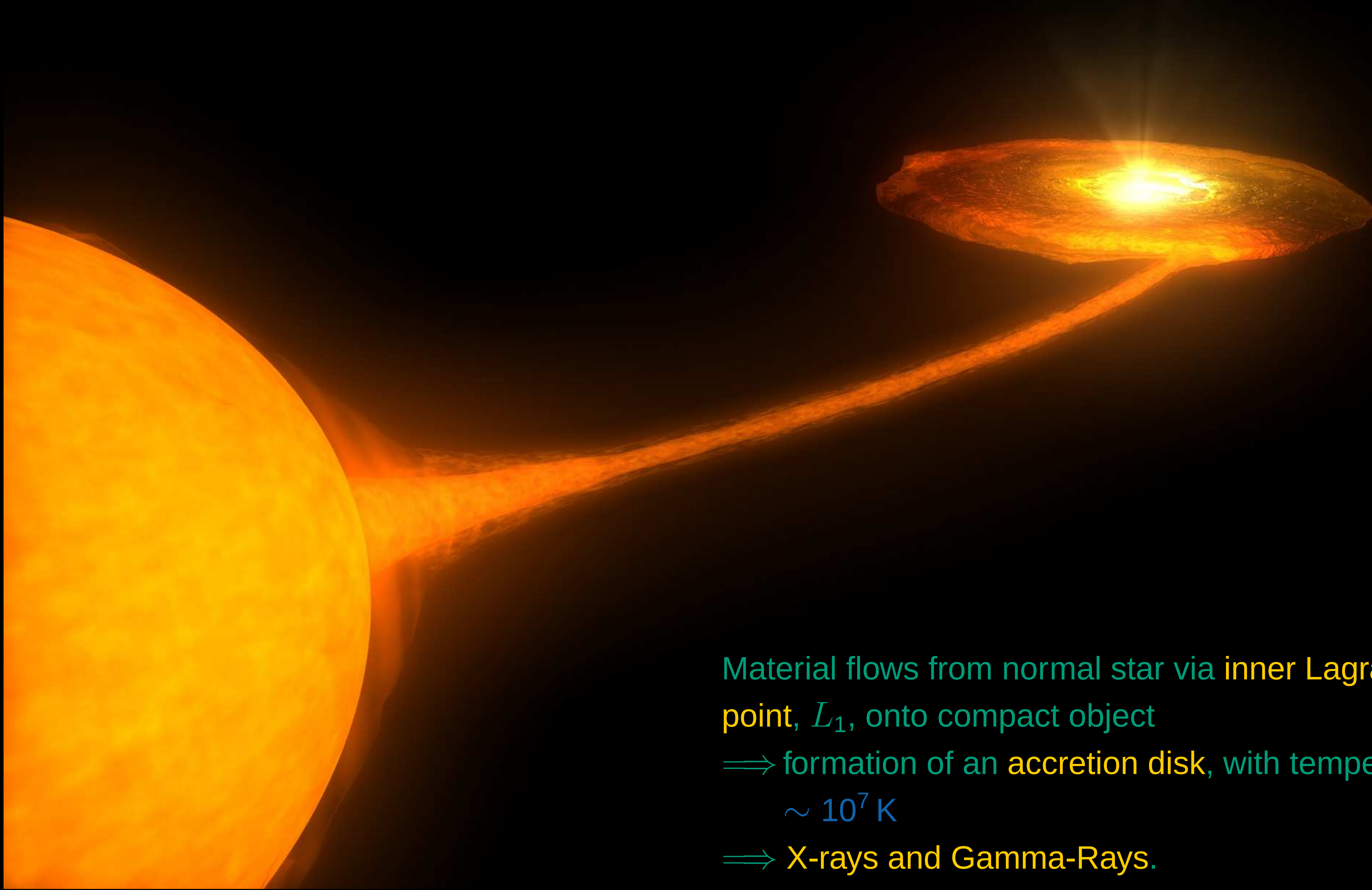

Material flows from normal star via inner Lagrange point, L_1, onto compact object

$\Longrightarrow$ formation of an accretion disk, with temperature $\sim 10^7$ K

$\Longrightarrow$ X-rays and Gamma-Rays.

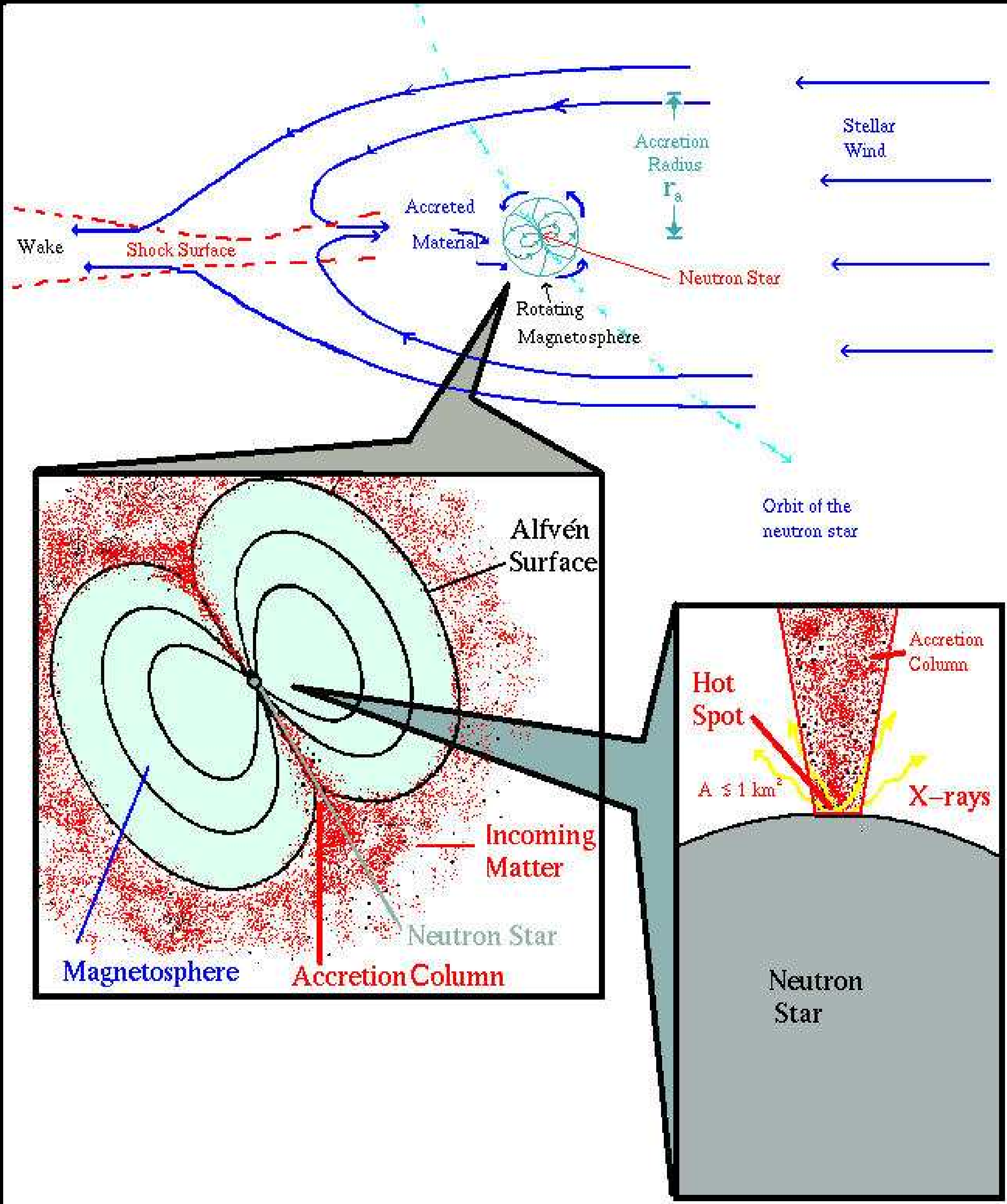

courtesy I. Negueruela, based on Davidson & Ostriker (1973)

X-Ray Binaries

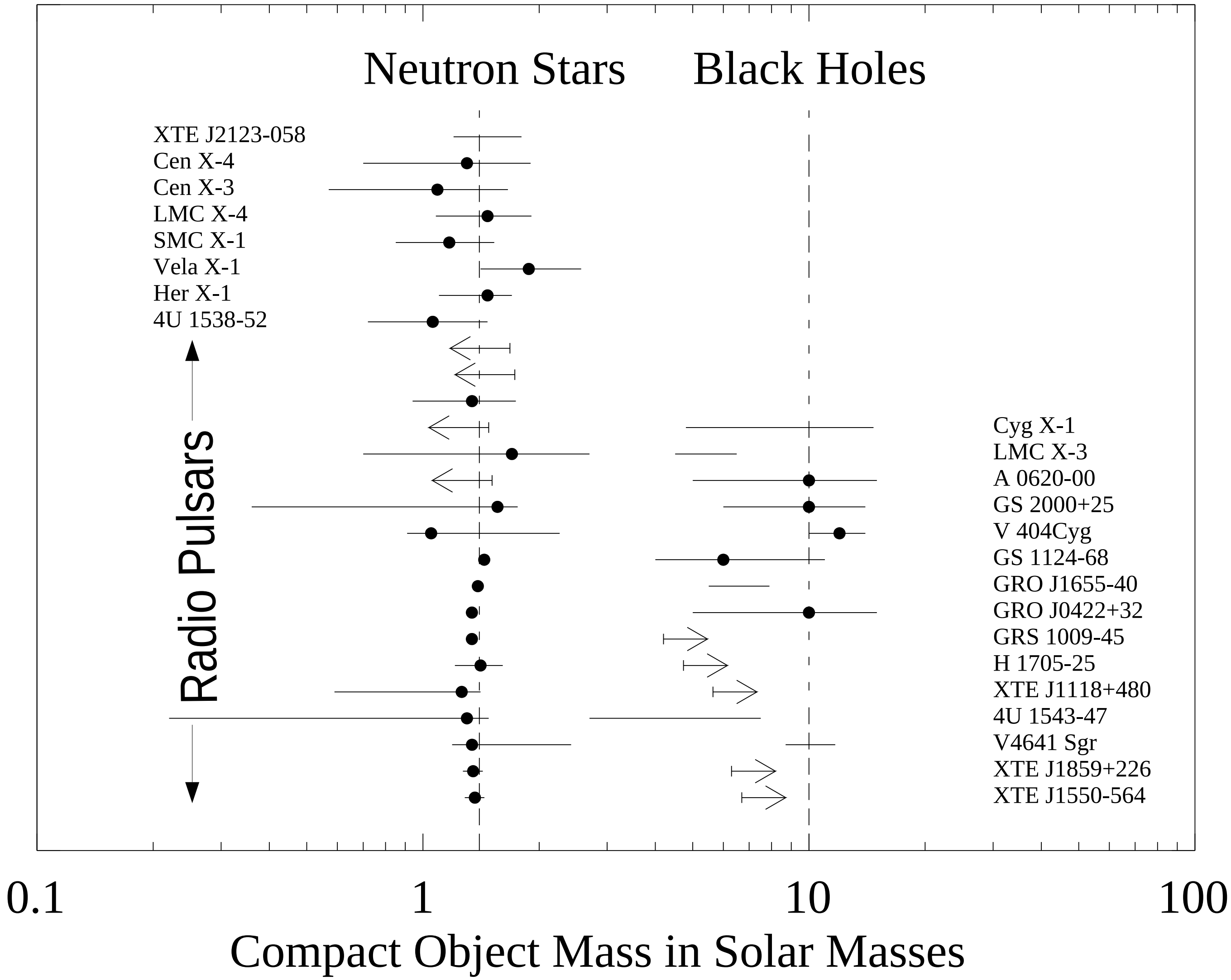

(Kalemci, priv. comm.)

X-ray binaries are neutron stars or black holes accreting material from a normal star.

Bahcall, J. N., & Bahcall, N. A., 1972, ApJ, 178, L1

Bowyer, S., Byram, E. T., Chubb, T. A., & Friedman, H., 1964, Nature, 201, 1307

Bowyer, S., Byram, E. T., Chubb, T. A., & Friedman, H., 1965, Science, 147, 394

Charles, P. A., & Seward, F. D., 1995, Exploring the X-Ray Universe, (Cambridge: Cambridge Univ. Press)

Davidson, K., & Ostriker, J. P., 1973, ApJ, 179, 585

Forman, W., Jones, C., Cominsky, L., Julien, P., Murray, S., Peters, G., Tananbaum, H., & Giacconi, R., 1978, ApJS, 38, 357

Giacconi, R., Gursky, H., Paolini, F. R., & Rossi, B. B., 1962, Phys. Rev. Lett., 9, 439

Hjellming, R. M., & Wade, C. M., 1971, ApJ, 168, L21

Murdin, P., & Webster, B. L., 1971, Nature, 233, 110

Schreier, E., Levinson, R., Gursky, H., Kellogg, E., Tananbaum, H., & Giacconi, R., 1972, ApJ, 172, L79

Tananbaum, H., Gursky, H., Kellogg, E. M., Levinson, R., Schreier, E., & Giacconi, R., 1972, ApJ, 174, L143

Walter, F. M., & Matthews, L. D., 1997, Nature, 389, 358

Webster, B. L., & Murdin, P., 1972, Nature, 235, 37

Accretion in X-Ray Binaries